

Rapid Sonochemical Synthesis and Characterisation of Copper Oxide Nanoparticles from Schweizer's Reagent

Huu Dang, Ravi Krishna Brundavanam, Gerrard Eddy Jai Poinern , Derek Fawcett

Murdoch Applied Nanotechnology Research Group, Department of Physics, Energy Studies and Nanotechnology, School of Engineering and Energy, Murdoch University, Murdoch, Western Australia 6150, Australia

Abstract: The present work reports the results of a study that investigated a sonochemical approach to synthesis copper oxide nanostructures from tetraamminediaquacopper dihydroxide. (Schweizer's Reagent). Ultrasonic irradiation ranging from 0 to 400 W over time periods ranging from 5 min to 15 min were performed on Schweizer's reagent. UV-visible spectroscopy has shown that copper nanoparticles are initially formed but soon oxidize in the ultrasonically treated reagent. Formation of copper oxide nanostructures was indicated by the original blue colour of the reagent turning brown at particular power settings. XRD analysis confirmed the presence of both copper (I) oxide (Cu_2O) and copper (II) oxide (CuO) at the end of the ultrasonic treatment. SEM microscopy revealed particles sizes ranged from 200 nm up to 1 μm and were predominantly granular and agglomerated in nature.

Keywords: Copper Oxide, Nanostructures, Sonochemical Synthesis, Ultrasounds

1. Introduction

Copper is an abundant metal with excellent thermal and electrical properties and because of its lower cost compared to noble metals such as gold and silver it has been extensively used in numerous industrial applications. However, in recent years there has been significant interest shown in developing one-dimensional (1-D) nanometre scale copper oxide materials. There are two forms of copper oxide, the first is the red coloured cuprous oxide [copper (I) oxide, Cu_2O] and the second is the black coloured cupric oxide [copper (II) oxide, CuO]. With the passage of time and in the presence of moist atmospheric air Cu_2O with time decomposes to CuO . Both copper oxides in bulk form tend to be antiferromagnetic, ferroelectric and are p-type semiconductors with band gap of 1.2 eV for CuO and 2.137 eV for Cu_2O respectively. Although other studies have shown that the band gap for CuO can range between 1.3 and 1.7 eV [1]. The band gap of both copper oxides makes them potential candidates for a number of applications such as solar cells, sensors electronic cathode materials, high temperature superconductors, optoelectronic devices and catalytic materials for converting hydrocarbons

into carbon dioxide and water [2-4]. In general nanometre scale materials have significant properties differences compared to their bulk counterpart and copper oxide one-dimensional structures such as nanowires also display unique properties. The properties are largely dependent the structures size, shape and surface chemistry. These unique properties are derived from the extremely large surface areas and large aspect ratios, which tend to promote surface interactions and processes. This makes one-dimensional copper oxide structures ideal candidates for chemical sensors [5, 6], photovoltaic devices and solar cells [7, 8]. And recent in years there has been many studies carried out using copper oxide nanowires to develop solar cells [9-11] and a wide range of chemical sensors [12], gas sensors [13], photo-electrochemical hydrogen generation [14] and catalytic oxidation of methane [15].

A wide range of techniques have been developed and used globally by researchers to synthesize copper oxide nanostructures. Techniques used to manufacture copper oxide nanostructures include wet chemical methods [16, 17], direct plasma [18], electrochemical [19], hydrothermal [20] and thermal

This article is published under the terms of the Creative Commons Attribution License 4.0

Author(s) retain the copyright of this article. Publication rights with Alkhaer Publications.

Published at: <http://www.ijsciences.com/pub/issue/2015-11/>

DOI: 10.18483/ijSci.863; Online ISSN: 2305-3925; Print ISSN: 2410-4477



Gerrard Eddy Jai Poinern (Correspondence)



g.poinern@murdoch.edu.au



+61 8 9360-2892; Fax: +61 8 9360-6183

oxidation [21, 22]. Among the wide range of synthesis techniques currently available, the use of ultrasound irradiation for the production of nanometre scale materials offers some unique reaction conditions which cannot be reproduced by the above-mentioned techniques.

During ultrasonic irradiation of a fluid medium, the alternating compressive and expansive acoustic waves create bubbles, which subsequently grow and ultimately undergo an implosive collapse. Throughout the growth period, the bubble accumulates ultrasonic energy until a critical size is reached, usually a few micrometres in size, before the bubble collapses. During the bubble implosion, the concentrated energy stored in the bubble is released within a very short duration producing a localized region of extremely high pressures and temperatures. The short-lived implosion can produce pressures of ~1000 bar and temperatures of ~5000 K, with heating and cooling rates greater than 10^{10} K s⁻¹ [23]. Interestingly, it is the transient nature of the acoustically produced cavitations, produced by the ultrasonic irradiation that generates the unique effects of ultrasound.

During the last decade there has been significant progress in synthesizing a wide variety of nanometre scale materials via sonochemical processes using a variety of ultrasound based techniques [23]. The sonochemical approach has a number of features that clearly distinguish it from conventional non-ultrasound based techniques. For most materials these features include: (1) faster primary nucleation; (2) relatively easy nucleation in materials that are usually difficult to nucleate otherwise; (3) the initiation of secondary nucleation; and (4) the production of smaller, purer crystals that are more uniform in size. It is due to these advantageous features that have made sonochemical synthesis an attractive technique for producing nanometre scale materials.

In the present paper, we report the synthesis of copper oxide nanostructures via a sonochemical technique that uses ultrasound irradiation as the driving mechanism in the process for Schweizer's reagent using ammonia as a base. The copper oxide nanostructures formed were subsequently investigated using advanced characterisation techniques such as X-ray diffraction (XRD) analysis to confirm the presence and type of copper oxides present, scanning electron microscopy (SEM) to determine particle size and morphology and UV-visible spectroscopy and Fourier Transform Infrared Spectroscopy (FT-IR) were used to monitor the formation of the nanostructures.

2. Materials and Methods

2.1. Materials

Analytical reagent grade Copper Sulphate

[CuSO₄·5H₂O] and Ammonium Chloride [NH₄Cl] were supplied by Chem Supply (Australia). Ajax Fine Chemicals supplied analytical grade Urea [CH₄N₂O] and Bio Lab supplied the (25% w/w) analytical reagent grade Ammonia solution. The glass microscope slides were supplied by Sail, while all aqueous solutions were prepared with Milli-Q[®] water (18.3 MΩ) produced by Thermo Scientific Water System (Barnstead Ultrapure System D11931).

2.2. Synthesis of copper oxide nanostructures

The procedure begins by preparing the glass microscope slides, which are used as sample substrates. Each glass slide was placed into Transtek[®] Systems Soniclean 30A (20 W) ultrasonic bath containing acetone and clean for 15 minutes at room temperature. After ultrasonic treatment the glass slide was rinsed using Milli-Q[®] water before being allowed to air dry. After drying the slides were then stored in airtight containers ready for use. A 1000 mL stock solution of Schweizer's reagent was used as the reactant mixture. The reagent consisted of a 50 ml solution of 0.01 M Urea, 400 ml solution of 0.01 M of CuSO₄·7H₂O, 50 ml solution of 25 % NH₃ and 500 ml solution of 0.02 M NH₄Cl. The ingredients were thoroughly mixed to produce a clear blue solution (0% power solutions) as seen in Figure 1 (b). The stock solution was then used to prepare three sets of test solutions. Each set consisted of a six small vials each containing 50 ml of the stock solution. In each set, one vial acted as the control and was not subjected to ultrasonic treatment. The glass slides were then placed into the vials and then subjected to varying amounts of ultrasonic power (20, 40, 60, 80 and 100 %), with 100 % being equivalent to 400 W. The ultrasonic power was supplied by a Hielscher Ultrasonic processor UP400S [400 W, 24 kHz, H22 Sonotrode (22 mm dia.)]. The power output was controlled via the rotary regular as per manufacturer's specification. The procedure was repeated for three time periods 5 min, 10 min and 15 min. During ultrasonic treatment UV-visible spectroscopy and Fourier Transform Infrared Spectroscopy (FT-IR) was used to monitor copper oxide nanostructure formation. After ultrasonic treatment the glass slides were rinsed using Milli-Q[®] water before being allowed to air dry and then stored in airtight containers ready for further advanced characterisation.

2.3. Advanced characterisation

UV-visible spectroscopy was carried out after each set of ultrasonic treatments to monitor copper oxide nanostructure formation. Samples were examined using a UV-Visible spectrophotometer (Varian Cary 50 series, V3) over a spectral range from 200 nm up to 1100 nm (1 nm resolution) at room temperature (24 °C). A Perkin-Elmer Frontier Fourier Transform Infrared (FT-IR) spectrometer fitted with a Universal Single bounce Diamond ATR attachment (Range:

525 cm^{-1} to 4000 cm^{-1} in 4 cm^{-1} increments) was used to investigate functional groups and vibration modes present in the samples. A GBC[®] eMMA X-ray Powder Diffractometer [Cu $K\alpha$ = 1.5406 Å radiation source] was used to carry out the diffraction study and identify copper oxide phases present in the samples. The Diffractometer operated at 35 kV and 28 mA in flat plane geometry mode with each scan taking 2 seconds, while the diffraction patterns were collected over a 2θ range of 20° to 90° . A Cressington 208HR High Resolution Sputter coater was used to sputter coat samples with a 2 nm layer of gold to prevent charge build prior to Scanning electron microscope (SEM). SEM micrographs were taken using a JCM-6000 (NeoScopeTM) to determine size and morphology of copper oxide nanostructures formed.

3. Results and Discussions.

3.1. Ultrasonic Treatment of Schweizer's Reagent and Spectroscopy Analysis

The experimental setup was designed around a Hielscher UP400S Ultrasonic processor as shown in Figure 1 (a). In turn, individual vials were placed on the sample tray and the sonotrode was lowered into the reagent. This was followed by the step of selecting a particular power setting and then switching on the processor. The ultrasonic treatment of each respective vial was carried out at various power settings and treatment periods as detailed in Figure 1 (b). The treatment was carried out at room temperature (24°C), however during treatment solutions temperatures reached 85°C . The vial on the extreme left was the control and was not subjected to ultrasonic treatment.

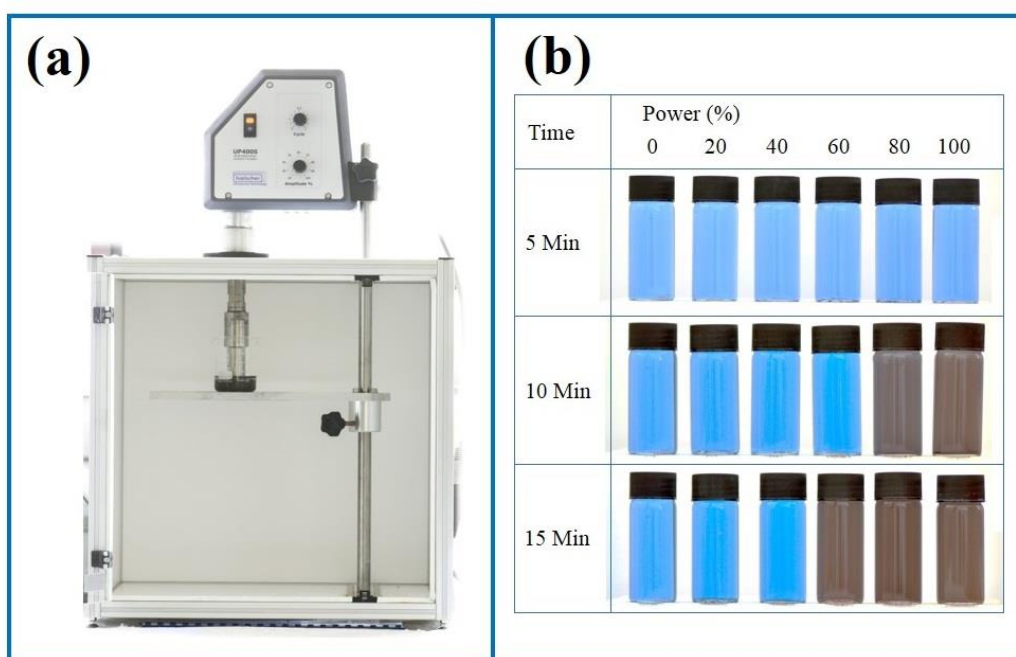


Figure 1. (a) Experimental setup showing ultrasonic processor and (b) Visual results of ultrasonic treatment of Schweizer's reagent over various powers and periods

Visual inspection of Figure 1 (b) reveals that during the 5 min treatment period there was no significant difference between all the samples including the control on the left (0 %). During the 10 min treatment periods, ultrasonic powers of 80 % (320 W) and above produced a visual colour change in the reagent. The reagent changed from a clear light blue to a brown colour. For 15 min treatment periods, powers of 60 % (240 W) and above produced a similar colour change. Furthermore, shining a red led laser through the solutions produced the typical Tyndall effect indicating the presence of nanoparticles suspended in the solution. Representative UV-Vis spectra for

solutions subjected to ultrasonic treatment for 5 min and 15 min is presented in Figure 2. Inspection of Figure 2 (a) reveals the presence of major peaks located at 375 nm, 560nm and 785 nm, which indicate the formation of copper nanoparticle of various sizes and morphologies [24]. However, the ultrasonic induced oxidation processes produced in the reaction solution results in the rapid oxidation of the newly formed copper nanoparticles. Inspection of Figure 2 (b) reveals the presence of strong broadening of the plasmon resonances between 450 nm to 660 nm indicating the formation copper oxide nanoparticles [25].

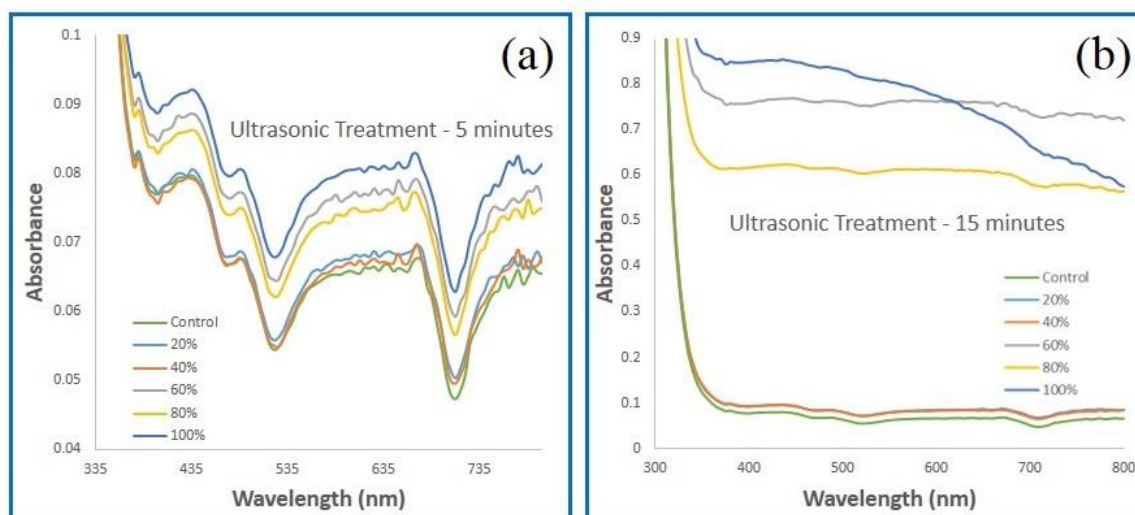


Figure 2. UV-visible spectroscopy analysis of ultrasonic treatments for 5 min and 15 min showing the initial formation of copper nanoparticles followed by their rapid oxidation to form copper oxide nanostructures

Figure 3 (a) presents a representative FT-IR analysis of a 15 min ultrasonic treatment at 100 % power. The wavelength of the respective absorption bands and their corresponding assignments are tabulated in Figure 3 (a). In summary, starting from the right hand side of Figure 3 (a), the analysis reveals the presence of a broad absorption band extending from 3700 to 3000 cm^{-1} and corresponds to O-H stretching [26]. The strong and broad band centred around 1274 cm^{-1} and the band located at 1073 cm^{-1} can be assigned to sulphate absorptions (ν_3) and (ν_1) respectively. While the bands located at 905, 933, 894, 854 and 675 cm^{-1} are due to sulphate compounds [27-28].

3.2 XRD analysis and SEM studies

XRD analysis was carried out on the respective samples and a representative spectrum for 15 min and 100 % ultrasonic power is presented in Figure 3 (b). Inspection of Figure 3 (b) reveals that the peaks are predominantly copper oxide species. There are three very weak peaks in the diffraction pattern occurring at 42.4°, 51.0° and 74.3° that correspond to the [111], [200] and [220] planes of the FCC structure of copper. This result confirms the results of the UV-visible spectroscopy analysis for a 15 min ultrasonic treatment, in which the treatment significantly creates a highly oxidizing environment that rapidly oxidizes copper nanoparticles.

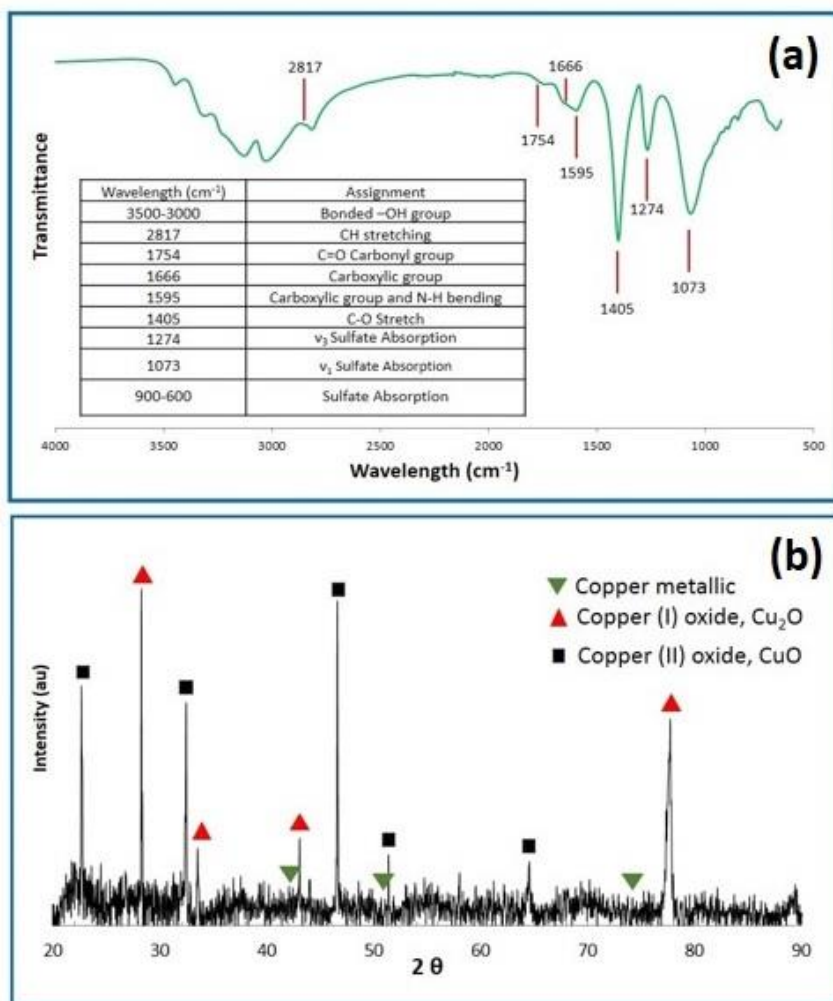


Figure 3. (a) Representative FT-IR analysis of a 15 min ultrasonic treatment and (b) representative XRD diffraction spectrum of a 15 minute ultrasonic treatment

Inspection of Figure 3 (b) also reveals the presence of peaks located at 29.2°, 36.4°, 42.0° and 76.3° which correspond to the [110], [111], [200], and [222] structures of copper (I) oxide (Cu₂O) are indicated by red triangles. The peaks located at 32.4°, 48.2°, 52.6° and 66.4° correspond to the [-111], [-202], [020], and [-311] structures of copper (II) oxide (CuO) are indicated by black squares. The XRD analysis confirms the formation Cu⁰, Cu₂O and CuO in the diffraction patterns of the sample powders. However, because of the highly oxidizing atmosphere created in the ultrasonic field, the initially formed copper nanoparticles are rapidly oxidized. The procedure ultimately results in both Cu₂O and CuO being the end products of the sonochemical reaction. Representative XRD patterns were used to determine copper oxide crystalline sizes ($t_{(hkl)}$) using the Debye-Scherrer equation [29, 30] where, λ is the wavelength

of the monochromatic X-ray beam, B is the Full-Width at Half Maximum (FWHM) of the peak at the maximum intensity, $\theta_{(hkl)}$ is the peak diffraction angle that satisfies Bragg's law for the (h k l) plane and $t_{(hkl)}$ is the crystallite size.

$$t_{(hkl)} = \frac{0.9\lambda}{B \cos \theta_{(hkl)}} \quad (1)$$

Analysis has revealed that time didn't have any major effect on crystallite size, but the level of ultrasonic power used during the treatment did influence crystallite size. Increasing ultrasonic power tended to reduce the size of the crystallites, with sizes ranging from 8 nm down to 72 nm as the power varied from 400 W (100 %) down to 80 W (20 %) respectively.

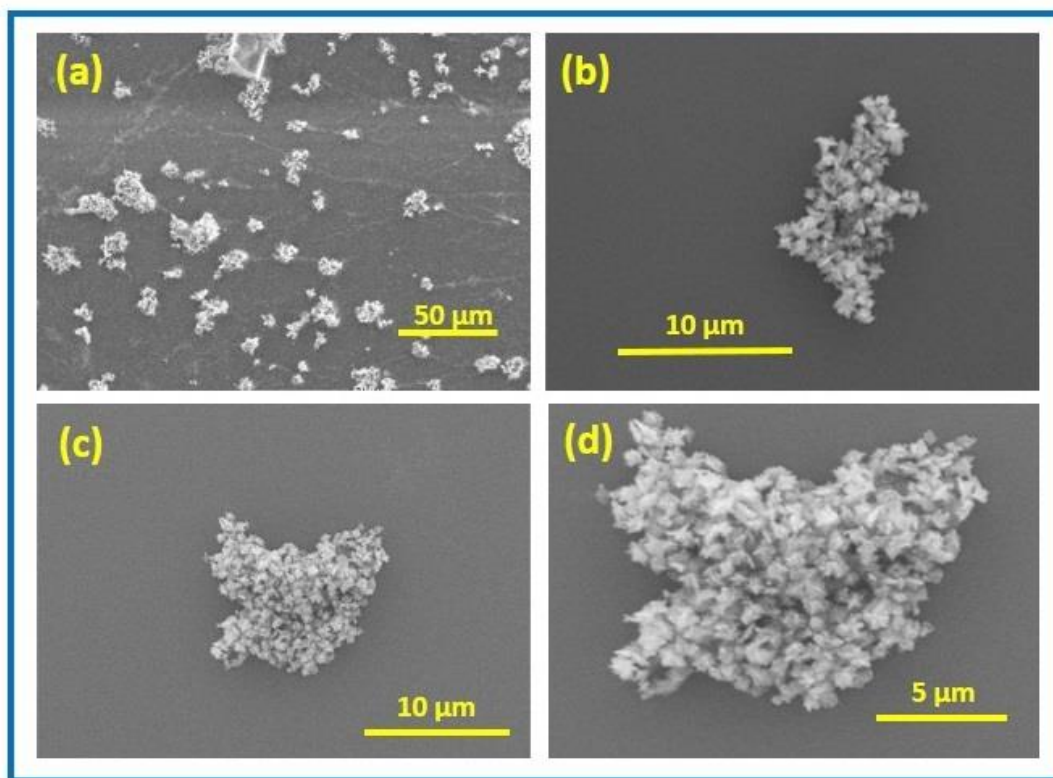


Figure 4. (a) Overview of copper oxide nanoparticle aggregations; (b) and (c) are enlarged views of representative agglomerations; and (d) enlarged view of granular, plate-like and rod-like morphologies present in the agglomerations

Microscopy studies using (SEM) reveals the particle size and morphology of the particles produced during ultrasonic treatment. Figure 4 presents a representative micrograph of copper oxide nanoparticle produced via a 15 minutes period at 400 W (100 %). Micrograph reveals an array of agglomerations scattered over the substrate surface. While the enlarged image presented in Figure 4 (b) reveals that the agglomerations are composed of numerous particles with granular and some rod-like nanostructures.

The ultrasonic treatment has been able to synthesis copper oxide nanostructures with particle size control achieved through the power setting. The nanoparticles are predominantly granular in nature with some plate-like and rod-like structures in smaller numbers as seen in Figure 4 (d), with particles ranging in size from around 200 nm up to around 1 μ m. Future studies are planned to further investigate the ultrasonic processes and to optimise the experimental parameters and improve the yield of copper oxide nanostructures.

Conclusion

The present investigation has shown that a sonochemical approach using ultrasonic irradiation was capable of producing copper oxide nanostructures directly from Schweizer's reagent

(tetraamminediaquacopper dihydroxide). The ultrasonic power was varied between 0 to 400W over time periods ranging from 5 min to 15 min. The reaction produced the initial blue colour of the reagent to turn brown. UV-visible spectroscopy revealed that copper nanoparticles were formed initially, but rapidly oxidized in the highly oxygenated ultrasonically induced reagent. Subsequent XRD analysis revealed the presence of both copper (I) oxide (Cu₂O) and copper (II) oxide (CuO) particles after synthesis. While analysis of the SEM microscopy data revealed the copper oxide particles ranged in size from 200 nm up to 1 μ m and were predominantly granular in nature with some rod-like structures present in smaller numbers. The results of this study are very promising as a facile method and further studies are planned to investigate the nucleation process more closely and optimise the experimental parameters to improve the yield from the sonochemical process.

Acknowledgements

The authors would like to thank Mrs Mona Shah and Mr Ken Seymour for their assistance in the laboratory.

Disclosure

The authors report no conflict of interest in this work.

References

- Filipič, G., and U. Cvelbar. 2012. Copper oxide nanowires: a review of growth. *Nanotechnology*. 23 (19), 194001.
- Sunkara, M. K., Pendyala, C., Cummins, D., Meduri, P., Jasinski, J., Kumar, V., Russell, H. B., Clark, E.L., Kim, J. H. 2011. Inorganic nanowires: a perspective about their role in energy conversion and storage applications. *J. Phys. D: Appl. Phys.* 44: 174032, 1-9.
- Zhang, J., Liu, J., Peng, Q., Wang, X., Li, Y. 2006. Nearly mono-dispersed Cu₂O and CuO nanospheres: preparation and applications for sensitive gas sensors. *Chem. Mater.* 18(4): 867-871.
- Zhang, X., Wang, G., Liu, X., Wu, J., Li, M., Gu, J., Liu, H., Fang, B. 2008. Different CuO nanostructures: synthesis, characterisation, and applications for glucose sensors. *J. Am. Chem. C.* 112(43): 16845-16849.
- Cvelbar, U.K., Ostrikov, K., Drenik, A., Mozetic, M. 2008. Nanowire sensor response to reactive gas environment. *Applied Physics Letters*. 92:133505.
- Meyyappan, M. 2009. Catalyzed chemical vapor deposition of one-dimensional nanostructures and their applications. *Progress in Crystal Growth and Characterization of Materials* 55 (1-2): 1-21.
- Akimov, Y.A, Ostrikov, K., Li, E.P. 2009. Surface Plasmon Enhancement of Optical Absorption in Thin-Film Silicon Solar Cells” *Plasmonics* 4(2):107-113.
- Seo, D.H., Rider, A.E., Arulsamy, A.D., Levchenko, I., Ostrikov, K. 2010. Increased size selectivity of Si quantum dots on SiC at low substrate temperatures: An ion-assisted self-organization approach. *Journal of Applied Physics*. 107: 024313.
- Wang, Y., Shen, R., Jin, X., Zhu, P., Ye, Y., Hu, Y. 2011. Formation of CuO nanowires by thermal annealing copper film deposited on Ti/Si substrate.” *Applied Surface Science* no. 258 (1):201-206. doi: <http://dx.doi.org/10.1016/j.apsusc.2011.08.031>.
- Yuhas, B.D, Yang, P. 2009. Nanowire-Based All-Oxide Solar Cells. *Journal of the American Chemical Society* 131(10): 3756-3761. doi 10.1021/ja8095575.
- Raksa, P., Nilphai, S., Gardchareon, A., Choopun, S. 2009. Copper oxide thin film and nanowire as a barrier in ZnO dye-sensitized solar cells. *Thin Solid Films*. 517 (17): 4741-4744.
- Zappa, D., Comini, E., Zamani, R., Arbiol, J. Morante, R., Sberveglieri, G. 2013. Preparation of copper oxide nanowire-based conductometric chemical sensors. *Sensors and Actuators B: Chemical*. 182: 7-15. doi: <http://dx.doi.org/10.1016/j.snb.2013.02.076>.
- Hoa, N. D., Quy, N.V., Jung, H., Kim, D., Kim, H., Hong, S.K. 2010. Synthesis of porous CuO nanowires and its application to hydrogen detection. *Sensors and Actuators B: Chemical*. 146 (1): 266-272. doi: <http://dx.doi.org/10.1016/j.snb.2010.02.058>.
- Hsu, Y.K., Yu, C.H., Lin, H.H., Chen, Y.C., Lin, Y.G. 2013. Template synthesis of copper oxide nanowires for photoelectrochemical hydrogen generation. *Journal of Electroanalytical Chemistry*. 704: 19-23. doi: <http://dx.doi.org/10.1016/j.jelechem.2013.06.008>.
- Yunzhe, F., Rao, P.M., Kim, D.R., Zheng, X. 2011. Methane oxidation over catalytic copper oxides nanowires. *Proceedings of the Combustion Institute*. 33 (2): 3169-3175. doi: <http://dx.doi.org/10.1016/j.proci.2010.05.017>.
- Ethiraj, A.S., Kang, D.J., 2012. Synthesis and characterisation of CuO nanowires by a simple wet chemical method. *Nanoscale Research letters*. 7(70): 1-5
- Wang, W., Zhuang, Y., Li, L. 2008. Structure and size effect of CuO nanowires prepared by low temperature solid-phase process. *Mater. Lett.* 62(10-11): 1724-1726.
- Chen, Z., Cvelbar, U., Mozetič, M., He, J., Sunkara, M. K. 2008. Long range ordering of oxygen-vacancy planes in α -Fe₂O₃ nanowires and nanobelts. *Chem. Mater.* 20 3224-3228.
- Shin, H.S., Song, J.Y., Yu, J. 2009. Templated-assisted electrochemical synthesis of cuprous oxide nanowires. *Mater. Lett.* 63: 397-399.
- Li, C., Yin, Y., Hou, H., Fan, N., Yuan, F., Shi, Y., Meng, Q. 2010. Preparation and characterisation of Cu(OH)₂ and CuO nanowires by the coupling route of microemulsion with homogenous precipitation. *Solid State Commun.* 150: 585-589.
- Poinern, G.E.J., Dang, H., Brundavanam, R.K., Fawcett, D. 2014.
- Vertically aligned CuO nanometre scale wires synthesized by thermal oxidation in atmospheric air. *International Journal of Science*. 3 (7): 43-50.
- Hansen, B.J, Lu, G., Chen, J. 2008. Direct Oxidation Growth of CuO Nanowires from Copper-Containing Substrates, *Journal of Nanomaterials*. Article ID 830474, 1-11.
- Yasui, K. *Fundamentals of Acoustic Cavitation and Sonochemistry: In Theoretical and Experimental Sonochemistry Involving Inorganic Systems*. (Ed) Pankaj and Ashokkumar. (Pub) Springer Dordrecht Heidelberg London New York. doi: 10.1007/978-90-481-3887-6
- Khatoun, U.T., Rao, N.G., Mohan, M.K. 2013. Synthesis and characterisation of copper nanoparticles by chemical reduction method. *Proc. International conference on Advanced Nanomaterials & Emerging Engineering Technologies (ICANMEET-2013)*, New Delhi, India.
- Banejee, S. and Chakravorty, D. 2000. Optical absorption by nanoparticles of Cu₂O. *Europhysics Letter*. 52 (4): 468-473.
- Nakamoto, K. 1978. *Infrared and Raman Spectra of Inorganic and Coordination Compounds*, Wiley, New York, pp. 103-110.
- Serna, C.J., White, J.L., Hem, S.L. 1977. Anion-Aluminum Hydroxide Interactions. *Soil Sci. Soc. Am. J.* 42: 1009-1013. http://www.chemicalbook.com/SpectrumEN_7758-99-8_IR1.htm
- Danilchenko, S.N., Kukharenko, O.G., Moseke, C., Protsenko, I.Y., Sukhodub, L.F., Sulkio-Cleff, B. 2002. Determination of the bone mineral crystallite size and lattice strain from diffraction line broadening. *Crystal. Res. Technol.* 37 (11): 1234-1240.
- Klug, H.P., Alexander, L.E. 1974. *X-ray diffraction procedures for polycrystallite and amorphous materials*. 2nd edition. Wiley, New York, USA.